Improving Effectiveness and Performance Based on Dimensionality Reduction of CCD Image Features in Fall Armyworm's Control

Alex B. Bertolla [1,2] and Paulo E. Cruvinel [1,2]
[1]Embrapa Instrumentation, São Carlos, SP, Brazil
[2]Federal University of São Carlos - Post Graduation Program in Computer Science, São Carlos, SP, Brazil
E-mails: alex.bertolla@embrapa.br, paulo.cruvinel@embrapa.br

***Abstract*—The pest control in agriculture based on digital imaging sensors has increased significantly in the past decades. Such a strategy has become possible due to the continuous improvements in computational intelligence and machine learning techniques. However, the demand for analyzing and processing such an amount of data generated by these sensors has become a challenge due to the high dimensionality. This article presents a study on the dimensionality reduction of features from digital images acquired with a Charge-Coupled Devices sensor in an agricultural field, to choose the optimal number of principal components for reducing feature dimensionality. It also presents a machine-learning method for the pattern recognition of this species of caterpillar (Fall armyworms - *Spodoptera frugiperda*) in its different growth stages. In such a context, selecting the optimal number of principal components for dimensionality reduction, retaining only the necessary information associated with the main variables that describe the object of interest. The results have shown that using Hu invariant moments for feature extraction, dimensionality reduction was possible for all analyzed cases, leading to 80% of the original data. In this context, it was possible to preserve the semantic characteristics collected by the sensor. Support Vector Machine classifiers have reached more than 70% of accuracy and more than 80% of precision. Moreover, the performance of the classifiers was 30% faster when working with the dimensionality reduced of the feature vector than when working with the original data.**

Keywords-ccd sensor; digital image; feature extraction; dimensionality reduction; principal component analysis.

I. Introduction

In agriculture pest control plays an important role. In maize production, the Fall armyworm (*Spodoptera frugiperda*) has been requiring special attention, since it sponsors significant losses in production. In such a context, a previous study has been presented at the Ninth International Conference on Advances in Sensors, Actuators, Metering and Sensing (ALLSENSORS 2024) [1].

Charge-coupled devices (CCD) are the most used imaging sensors for digital image acquisition. They have built-in frame capture systems and the analog-to-digital conversion is done in the sensor itself [2].

CCD's sensors have been used in such ways to acquire images for different purposes. In agriculture, those sensors are usually used to capture images of pests and diseases [3] [4].

Due to the complex and high dimensions of the data captured by those sensors, storing and processing the amount of data acquired has become a challenging task [5], known as the curse of dimensionality [6]. This phenomenon is related to the fact, that with a certain degree of accuracy from a function estimation, the number of variables increases as the number of samples also has to increase [7].

To solve the issue of the curse of dimensionality, different methods based on dimensionality reduction techniques have been proposed [8]. These methods transform the original high-dimensional data into a new reduced dataset, removing the redundant and non-relevant features [9]. Dimensionality reduction algorithms allow an efficient reduction of the number of variables, and if applied before machine learning models can avoid overfiting.

In the literature, it is possible to find several available researches about dimensionality reduction techniques for different types of data, such as Principal Component Analysis (PCA) introduced in 1901 by Karl Pearson [10], and its variations [11], Linear Discriminant Analysis (LDA) [12], Singular Value Decomposition (SVD) [13] and Isometric Mapping (ISOMAP) [14], a non-linear dimensionality reduction method based on the spectral theory, which tries to preserve the geodesic distances in the lower dimension.

PCA is a linear dimension reduction technique and is the most predominant method applied [15], and was considered to compose this work.

This paper presents a method for dimensionality reduction optimization when using CCD sensor-based images to control Fall armyworms in agriculture. In fact, the task of image classification allows the machine to understand what type of information is contained in an image, on the other hand, semantic segmentation methods allow the precise location of different kinds of visual information, as well as each begins and ends. Besides, it also presents a case study based on selecting Support Vector Machine (SVM) classifiers to evaluate the reduced features and their relation with the original data.

After the introduction, the remainder of the paper is organized as follows: Section II describes the work methodology; Section III shows the results, Section IV the discussion of the experiments; and finally, Section IV presents the conclusion of this paper and suggestions for future works.

II. METHODS

All the experiments have been performed in Python, i.e., by using both the image processing and machine learning libraries in openCV, as well as scikit-image and scikit-learn algorithms respectively. We also have considered an operating platform with a 64-bit CPU Intel (R) model Core(TM) i7-970, 16Gb RAM, and operational system Microsoft Windows 11.

A. Digital Image Sensor and Dataset

A digital image can be defined as a bi-dimensional function $f(x, y)$, where (x, y) are the intensity positions, defined as pixel [16]. CCD's sensors can capture images in different color spaces, however, the most common color space is the Red Green, and Blue (RGB), representing the visible spectrum [17].

Table I presents the features of the images acquired using the CCD sensor.

TABLE I
IMAGE FEATURES ACQUIRED BY CCD SENSOR

Image type	JPG / JPEG
Color space	RGB
Width	3072 pixels
Height	2048 pixels
Resolution	72 pixels per inch (ppi)
Pixel size	0.35mm

Regarding the image acquisition, a dataset was generated using a CCD sensor. This dataset is composed of the Fall armyworm images in real maize crops, where the pest was found both in leaves and cobs maize.

B. Feature Extraction

The Hu invariant moments descriptor was considered for the extraction of the geometric features of the pest. For the calculation of the seven invariant moments of Hu, it is necessary, a priori, to calculate the two-dimensional moments, that is, the central moments and normalized central moments [18]. Two-dimensional moments are understood to be the polynomial functions projected onto a 2D image, $f(x, y)$, and size $M \times N$ and order $(p + q)$.

The normalized central moments allow the central moments to be invariant to scale transformations, being defined by:

$$\eta_{pq} = \frac{\mu_{pq}}{\mu_{00}^{\gamma}} \quad for \quad \mu_{00} \neq 0 \tag{1}$$

where γ is defined as:

$$\gamma = \frac{p+q}{2} + 1 \tag{2}$$

for $p + q = 2, 3, ...,$ positive integers $\in \mathbb{Z}$.

In this way, the invariant moments can be calculated considering:

$$\phi_1 = \eta_{20} + \eta_{02} \tag{3}$$

$$\phi_2 = (\eta_{20} - \eta_{02})^2 + 4\eta_{11}^2 \tag{4}$$

$$\phi_3 = (\eta_{30} - 3\eta_{12})^2 + (3\eta_{21} - \eta_{03})^2 \tag{5}$$

$$\phi_4 = (\eta_{30} + \eta_{12})^2 + (\eta_{21} + \eta_{03})^2 \tag{6}$$

$$\begin{gathered}\phi_5 = (\eta_{30} - 3\eta_{12})(\eta_{30} + \eta_{12}) \\ [(\eta_{30} + \eta_{12})^2 - 3(\eta_{21} + \eta_{03})^2] + \\ (3\eta_{21} - \eta_{03}) \\ (\eta_{21} + \eta_{03}) \\ [3(\eta_{30} + \eta_{12})^2 - (\eta_{21} + \eta_{03})^2]\end{gathered} \tag{7}$$

$$\begin{gathered}\phi_6 = (\eta_{20} - \eta_{02}) \\ [(\eta_{30} + \eta_{12})^2 - (\eta_{21} + \eta_{03})^2] + 4\eta_{11}(\eta_{30} + \eta_{12})\eta_{21} + \eta_{03})\end{gathered} \tag{8}$$

$$\begin{gathered}\phi_7 = (3\eta_{21} - \eta_{03})(\eta_{30} + \eta_{12}) \\ [(\eta_{30} + \eta_{12})^2 - 3(\eta_{21} + \eta_{03})^2] + \\ (3\eta_{12} - \eta_{30})(\eta_{21} + \eta_{03}) \\ [3(\eta_{30} + \eta_{12})^2 - (\eta_{21} + \eta_{03})^2]\end{gathered} \tag{9}$$

Neither of the seven Hu invariant moments is directly related to the size of an object in an image. However, the size of an object can be indirectly inferred through either the first or fourth moment [19].

After the features are extracted using the methods considered, a single feature vector is organized. Then, to reduce its dimensionality, PCA is applied [20].

C. Principal Components Analisys

PCA considers an array $\mathbf{X}$ of data with n samples representing the number of observations and m independent variables [21], that is:

$$\mathbf{X} = \begin{bmatrix} x_{11} & \cdots & x_{1m} \\ \vdots & \ddots & \vdots \\ x_{n1} & \cdots & x_{nm} \end{bmatrix} \tag{10}$$

Herein, the principal components are obtained for a set of m variables X_1, X_2, ..., X_m with means μ_1, μ_2, ..., μ_m and variance σ_1^2, σ_2^2, ..., σ_m^2, which are independent and have covariance between the n-th and m-th variable [9], in the form:

$$\mathbf{\Sigma} = \begin{bmatrix} \sigma_{11}^2 & \cdots & \sigma_{1m}^2 \\ \vdots & \ddots & \vdots \\ \sigma_{n1}^2 & \cdots & \sigma_{nm}^2 \end{bmatrix} \tag{11}$$

where $\mathbf{\Sigma}$ represents the covariance matrix. To do this, the pairs of eigenvalues and eigenvectors are found (λ_1, e_1), (λ_2, e_2), ..., (λ_m, e_m), where $\lambda_1 \geq \lambda_2 \geq ... \geq \lambda_m$ and associated with Σ [22], where the i-th principal component is defined by:

$$Z_i = e_{i1}X_1 + e_{i2}X_2 + ... + e_{im}X_m \tag{12}$$

where Z_i is the i-th principal component. The objective is to maximize the variance of Z_i, as:

$$Var(Z_i) = Var(e_i'\mathbf{X}) = e_i' Var(\mathbf{X}) e_i = e_i' \mathbf{\Sigma} e_i \tag{13}$$

where i = 1, ..., m. Thus, the spectral decomposition of the matrix $\mathbf{\Sigma}$ is given by $\mathbf{\Sigma} = \mathbf{P\Lambda P'}$, where $\mathbf{P}$ is the composite matrix by the eigenvectors of $\mathbf{\Sigma}$, and $\mathbf{\Lambda}$ the diagonal matrix of eigenvalues of $\mathbf{\Sigma}$ [23]. Thus, it has to be:

$$\mathbf{\Lambda} = \begin{bmatrix} \lambda_1 & 0 & \cdots & 0 \\ 0 & \lambda_2 & \cdots & 0 \\ \vdots & \vdots & \ddots & \vdots \\ 0 & 0 & \cdots & \lambda_m \end{bmatrix} \tag{14}$$

In general, the principal component of greatest importance is defined as the one with the greatest variance, which explains the maximum variability in the data vector. The second most important component is the component with the second highest variance, and so on, up to the least important component [13].

Likewise, the normalized eigenvectors represent the main components that constitute the feature vector with reduced dimension. Besides, such reduced components are used to describe the acquired images. Additionally, the reduced features are used for the recognition of the patterns of Fall armyworm (*Spodoptera frugiperda*), i.e., useful consideration for both cases, leaf or cob maizes.

D. Machine Learning and Pattern Recognition

The ability of a computational system to improve the performance of a task based on experience can be defined as machine learning (ML), performed through either supervised or unsupervised learning methods [24].

In such a context, the feature vector, with reduced dimensionality, was used such that the classification was considered according to its position in the feature space. Thus, groups composed of similar characteristics could be identified and classified using support vector machine (SVM) classifiers [25].

The SVM's classifier can be established based on linear behavior or even non-linear behavior. Classifiers with linear behavior use a hyperplane that maximizes the separation between two classes from a training dataset and their respective labels [26]. In this case, the hyperplane is defined by:

$$\mathbf{w} \cdot \mathbf{x} + b = 0 \tag{15}$$

where $\mathbf{w}$ is the normal vector to the hyperplane, $\mathbf{w} \cdot \mathbf{x}$ is the dot product of the vectors $\mathbf{w}$ and $\mathbf{x}$, and b is a fit term. Thus, Equation (16) divides the input space $\mathbf{X}$ into two regions, as follows:

$$\begin{array}{llll} \mathbf{w} \cdot \mathbf{x}_i + b \geq 1 & se & y_i = +1 \\ \mathbf{w} \cdot \mathbf{x}_i + b \leq 1 & se & y_i = -1 \end{array} \tag{16}$$

which can be summarized as:

$$y_i(\mathbf{w} \cdot \mathbf{x}_i + b) - 1 \geq 0, \quad \forall(\mathbf{x}_i, y_i) \in \mathbf{X} \tag{17}$$

Linearly separable datasets are classified efficiently by linear SVMs with some error tolerance with smooth margins. However, in several cases, it is not possible to efficiently classify training data using this modality of a hyperplane [26], requiring the use of interpolation functions that allow the operation in larger space, that is, using non-linear SVM classifiers.

In such a manner, SVMS can deal with non-linear problems through a $\mathbf{\Phi}$ function, mapping the dataset from its original space (input space) to a larger space (input space, characteristics) [27], characterizing a non-linear SVM classifier.

Besides, from the choice of Φ, the training data set $\mathbf{x}$, in its input space R^2 , is scaled to the feature space R^3, as:

$$\mathbf{\Phi}(\mathbf{x}) = \Phi(x_1, x_2) = (x^2, \sqrt[2]{2}x_1x_2, x_2^2), \tag{18}$$

$$\begin{array}{c} h(\mathbf{x}) = \mathbf{w} \cdot \mathbf{\Phi}(\mathbf{x}) + b = \\ w_1x_1^2 + w_2\sqrt[2]{2}x_1x_2 + w_3x_2^2 + b = 0 \end{array} \tag{19}$$

The data are initially mapped to a larger space, then a linear SVM is applied over the new space. A hyperplane is then found with a greater margin of separation, ensuring better generalization [28].

Thus, the classifier obtained becomes:

$$\begin{array}{c} g(x) = sgn(h(x)) = \\ sgn\left(\sum_{x_i \in SV} \alpha_i^* y_i \Phi(x_i) \cdot \Phi(x) + b^*\right) \end{array} \tag{20}$$

where b^* is calculated as:

$$\begin{array}{c} b^* = \frac{1}{n_{SV:\alpha^* < C}} \sum_{x_j \in SV:\alpha_j^* < C} \\ \left(\frac{1}{y_j} - \sum_{x_i \in SV} \alpha_i^* y_i \Phi(x_i) \cdot \Phi(x_j)\right) \end{array} \tag{21}$$

Given that the feature space can be in a very high dimension, the calculation of $\mathbf{\Phi}$ might be extremely costly, or even unfeasible. However, the only necessary information about the mapping is the calculation of the scalar products between the data in the feature space, obtained through function kernels [26].

Table II presents the kernels analyzed to validate the developed method.

TABLE II
SUPPORT VECTOR MACHINE FUNCTION KERNELS

Kernel	**Function** $K(x_i, x_j)$	**Parameters**
Polynomial	$(\delta(\mathbf{x}_i \cdot \mathbf{x}_j) + \kappa)^d$	δ, κ e d
Radial basis function kernel	$exp(-\sigma \left\|\mathbf{x}_i - \mathbf{x}_j\right\|^2)$	δ, κ e d
Sigmoidal	$\tanh(\delta(\mathbf{x}_i \cdot \mathbf{x}_j) + \kappa)$	δ e κ

The Radial basis function kernel (RBF), which is based on a Gaussian function, has been chosen for the ML process, to classify the Fall armyworm growth stage.

Accuracy and precision metrics have been measured for validation of the SVM classifiers, illustrated by both the confusion matrix and the receiver operating characteristic (ROC) curve.

III. RESULTS

Figure 1(a to e) illustrates one example of each stage of growth, also named Instar, Figure 1(f) illustrates two different Instar in the same image.

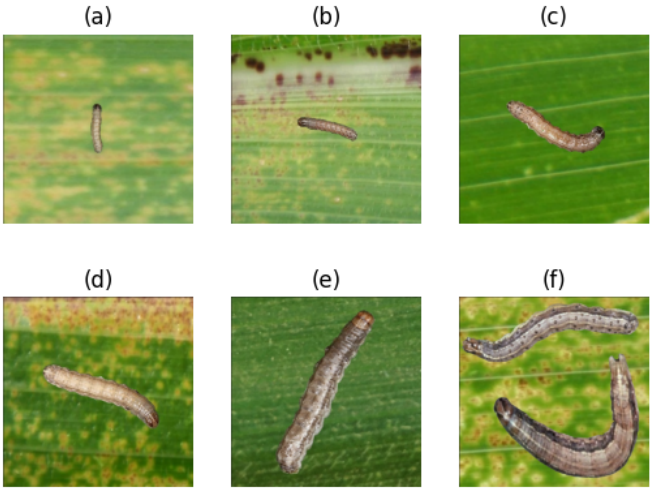

Figure 1. Fall armyworm (*Spodoptera frugperda*) in different stages of growth.

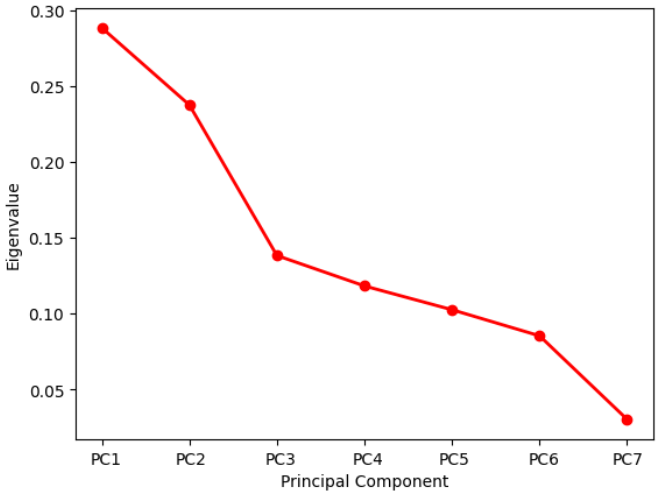

Figure 2. Scree plot.

TABLE III
FEATURE VECTOR COMPOSED OF HU INVARIANT MOMENTS. EXAMPLE OF THREE IMAGES

Hu invariant moments	Images		
	Image 1	Image 2	Image 3
ϕ_1	6.692	6.6178	6.524
ϕ_2	13.581	13.424	19.102
ϕ_3	24.321	23.944	22.370
ϕ_4	25.919	26.245	23.445
ϕ_5	51.517	-52.023	46.665
ϕ_6	34.307	-33.305	-34.728
ϕ_7	-51.458	-51.556	47.656

Table III presents the seven Hu invariant moments, as examples, from three different images, which were processed using the dataset.

Table IV presents the normalized seven Hu invariant moments from three different images.

TABLE IV
NORMALIZED FEATURE VECTOR. EXAMPLE OF THREE IMAGES

Hu invariant moments	Images		
	Image 1	Image 2	Image 3
ϕ_1	0.274	0.162	0.021
ϕ_2	-1.048	-1.121	1.496
ϕ_3	1.035	0.817	-0.092
ϕ_4	1.408	1.669	-0.575
ϕ_5	0.719	-1.607	0.610
ϕ_6	0.808	-1.289	-1.333
ϕ_7	-0.863	-0.865	1.199

Figure 2 shows the scree plot of the variance ratio.

Table V presents the maximum variance to each of the four principal components concerning the original data.

Figure 3 illustrates the maximum variance to each of the four principal components concerning the original data with the absolute values.

TABLE V
MAXIMUM VARIATION OF DATA IN RELATION TO EACH PRINCIPAL COMPONENT. BASED ON FOUR PRINCIPAL COMPONENTS.

Hu invariant moments	Principal components			
	PC 1	PC 2	PC 3	PC 4
ϕ_1	-0.147	-0.630	-0.120	-0.568
ϕ_2	0.501	-0.295	0.036	0.230
ϕ_3	-0.395	-0.424	0.087	0.027
ϕ_4	-0.378	0.501	-0.158	-0.479
ϕ_5	-0.376	-0.277	-0.310	0.286
ϕ_6	-0.355	-0.011	0.865	0.127
ϕ_7	0.398	-0.078	0.325	-0.543

Table VI presents the values of the four principal components.

TABLE VI
FEATURE VECTOR COMPOSED OF FOUR PRINCIPAL COMPONENTS. EXAMPLE OF THREE IMAGES

Principal components	Images		
	Image 1	Image 2	Image 3
PC1	0.333	2.121	-0.742
PC2	-2.280	-1.156	1.306
PC3	0.551	-1.243	-0.528
PC4	0.181	-1.193	0.012

The distribution of the variation of the four principal component values is illustrated in Figure 4.

This information can be observed in Figure 5, which illustrates a boxplot chart of the four principal component values and their distribution.

After the original data were reduced to two and four principal components, the experiments performed for classification considered SVM with a Gaussian function kernel, and the feature vector with reduced dimensionality was split into 70% for training and 30% for testing.

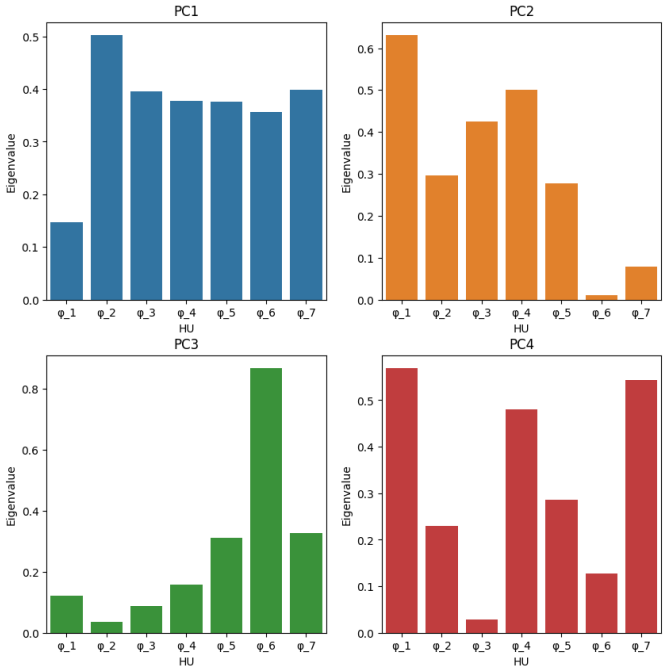

Figure 3. Maximum of data variation concerning each principal component, based on four principal components.

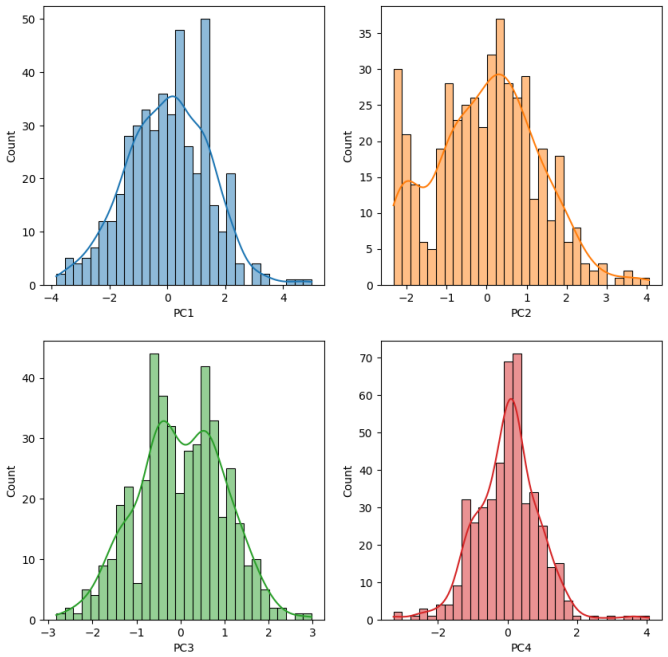

Figure 4. Histogram of distribution of the four principal components values.

Table VII presents the results of the classification of the five different stages of growth of the Fall armyworm based on four principal components.

Figure 6 illustrates the confusion matrix based on the data presented in Table VII.

Figure 7 illustrates the ROC curve based on the data presented in Table VII.

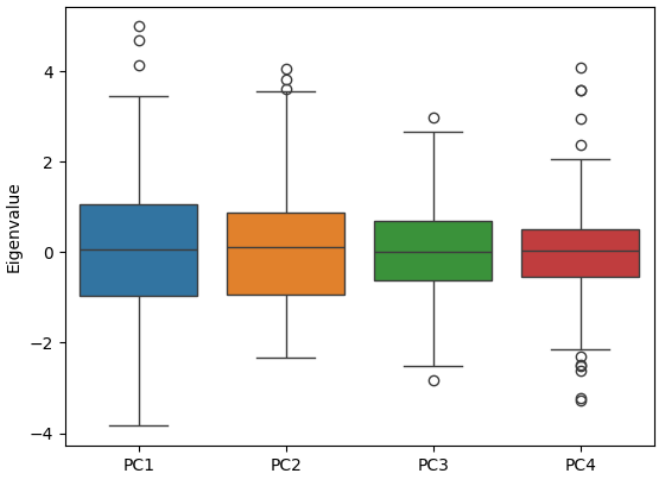

Figure 5. Boxplot of four principal components values.

TABLE VII
THE FALL ARMYWORM CLASSIFICATION RESULTS BASED ON FOUR PRINCIPAL COMPONENTS

Instar	Precision	Recall	F1-score
1	0.63	0.74	0.68
2	0.72	0.76	0.74
3	0.72	0.65	0.68
4	0.69	0.75	0.72
5	0.86	0.68	0.76

Based on the use of PCA the vector with the features for pattern recognition has been reduced in dimensionality, after that, the resultant vector was classified using an SVM classifier, i.e., having Gaussian kernel.

Table VIII presents the results of the classification of the five different stages of growth of the Fall armyworm.

TABLE VIII
THE FALL ARMYWORM CLASSIFICATION RESULTS BASED ON TWO PRINCIPAL COMPONENTS

Instar	Precision	Recall	F1-score
1	0.44	0.59	0.50
2	0.34	0.54	0.42
3	0.50	0.28	0.36
4	0.52	0.42	0.47
5	0.68	0.54	0.60

Figure 8 illustrates the confusion matrix based on the data presented in Table VIII.

Figure 9 illustrates the ROC curve based on the data presented in Table VIII.

The SVM classifier based on two principal components performed the classification of the five different stages of growth of the Fall armyworm with an accuracy of 47%.

Figure 10 illustrates the performance of the SVM classifier considering these selected components.

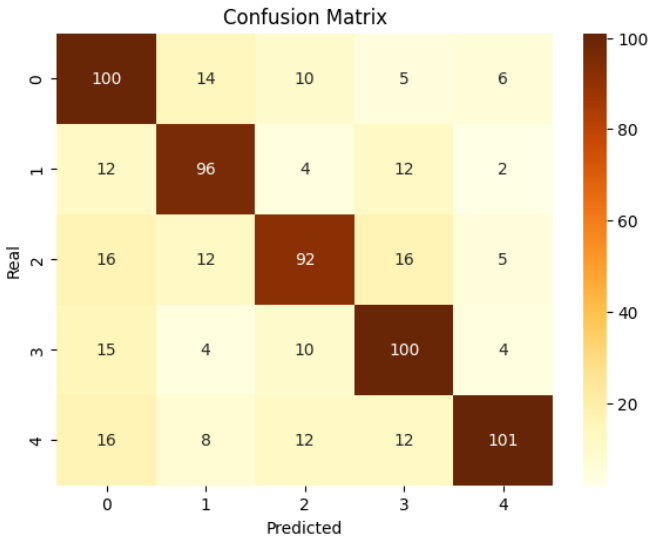

Figure 6. Confusion matrix for four principal components.

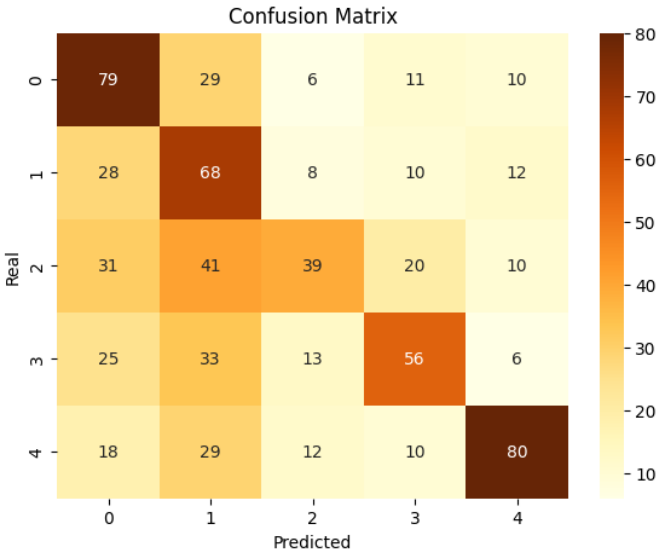

Figure 8. Confusion matrix for two principal components.

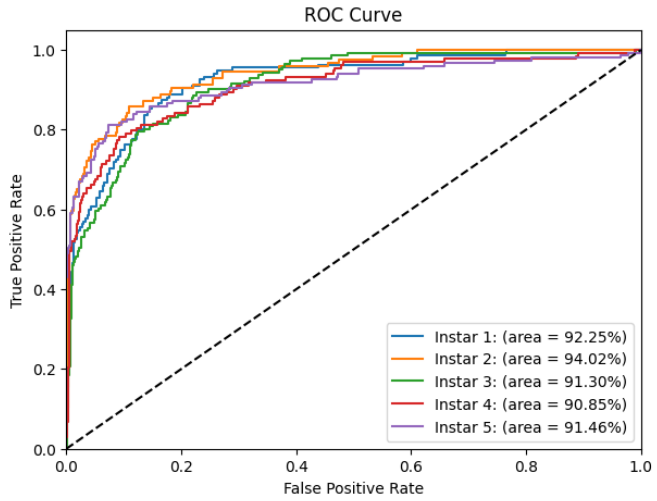

Figure 7. ROC curve for four principal components.

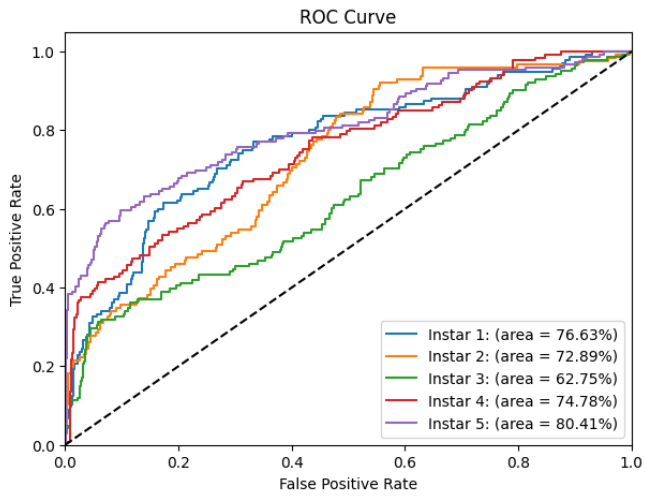

Figure 9. ROC curve for four principal components.

IV. Discussion

For this study, an image dataset composed of 2280 images acquired with CCD's sensor was used. These images represent the Fall armyworm (*Spodoptera frugperda*) acquired in a real environment of maize crop in its five different stages of growth, grouped in 456 images for each stage.

Considering all images contain at least one Fall armyworm in different stages, the Hu invariant moments descriptor has been considered for instance. Thus, for each image of the Fall armyworm, a feature vector was generated, containing the seven Hu invariant moments (ϕ_1, ϕ_2, ϕ_3, ϕ_4, ϕ_5, ϕ_6 and ϕ_7), which are related to the shape and geometrical features of this pest. The features contained in these vectors will allow the classification of the Fall armyworm (*Spodoptera frugperda*) in its different stages of growth.

As the values of the feature vectors were in different scales, it was necessary to normalize them. To generate a database of characteristics of the Fall armyworm (*Spodoptera frugperda*), the feature vectors referring to each image were saved on disk.

The remotion of duplicated and less significant information, based on the application of PCA, has allowed improvements in computational performance. In fact, the appropriate number of principal components that explain the original data were considered.

Therefore, it is possible to infer that by applying two to four principal components it is possible to explain almost 55% to 80% of the variability of the original data. Considering that, the experiments were based on four principal components.

As already discussed, neither of the seven invariant moments is directly related to the size of an object. However, the first and the fourth moments can be used to infer the size of

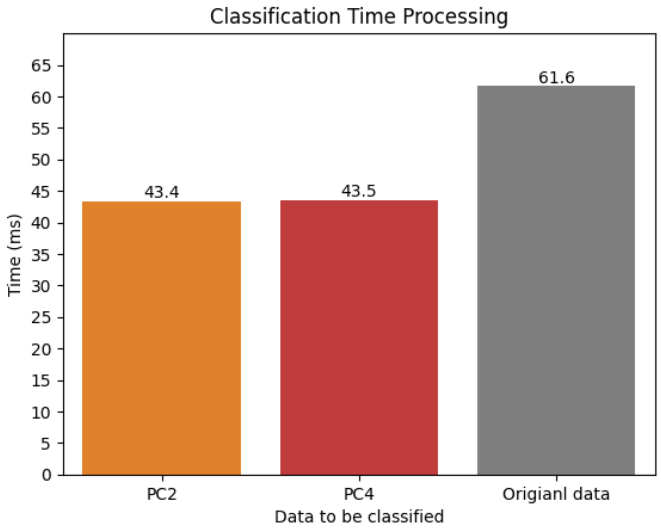

Figure 10. Classification time processing considering two and four principal components and the original data.

an object in an image.

Moreover, through the maximum variation ratio metric it is possible to measure the weight of each of Hu invariant moments in each principal component.

Even though the maximum variation ratio presents some negative values, the weights for each principal component are considered absolute values. For example, in PC2, the first moment (ϕ_1) has the highest weight.

The experiment with four principal components showed that, as can be visualized in Figure 3, to have the most representative weights either from the first moment or the fourth moment, it was necessary to work with two or four principal components.

The feature vector's dimensionality reduction was performed Based on prior experiments. Table VI presents the values of the four principal components.

Once the values of the four principal components are obtained, it is necessary to evaluate if it is sufficient to work with two principal components, or whether it should be considered four principal components. For this purpose, the maximum variation of each principal component should be considered concerning the original data, the extent to which the principal components could explain the original data and the minimum error.

This experiment demonstrated that working with four principal components was the ideal option. Because both the first and fourth moments are very representative, four principal components can explain 80% of the original data, and even with a low increase in the error, it is not considerable to decrease the estimation.

Furthermore, SVM classifiers with Gaussian function kernel have been considered for machine learning processes. Both accuracy and precision were taken into account to validate the classification of the Fall armyworm, with features vector dimensionality reduced.

The features vector composed of two and four principal components was split into two segments, one for training the SVM classifier with the proportion of 70% and the other one, with 30% for testing purposes.

Results obtained in the classification process with two principal components and illustrated in the ROC curve presented in Figure 9, showed the SVM classifier has performed satisfactorily, with the accuracy rate of 30% demonstrates that working with two principal components might have satisfactory performance for representing the original data, however, in the proposed scenario, the classification of the different stage of growth of the Fall armyworm with two principal components might not be enough.

On the other hand, when the classification process was performed with four principal components, the ROC curve illustrated in Figure 7 showed the classification of the five different stages the accuracy ratio assessed increased to 71%, obtained an efficient classification of patterns of the Fall armyworm.

Finally, Figure 10 shows the performance of the SVM classifiers in milliseconds to execute the testing of the dataset classification. As expected, the original feature vector took more time to be processed, 61.1 milliseconds, while the feature vector with reduced dimensionality took less time to be classified, 43.5 and 43.4 for PC4 and PC2, respectively.

V. Conclusion and Future Work

This paper presented a study of dimensionality reduction using Principal Components Analysis (PCA), considering feature vectors composed of extracted Hu invariant moments.

Before measuring the number of principal components necessary to represent the original data from the Fall armyworm digital images, the feature vectors were normalized, to obtain all the seven Hu invariant moments.

The measure of the explained variance ratio to the original data was applied to verify the quantity number of principal components necessary to explain the maximum of the original data.

In addition, the first and fourth invariant moments were used to infer the estimated size of the Fall armyworm (*Spodoptera frugperda*) in the images.

Likewise, the measure of the maximum variation of each principal component, concerning each Hu invariant moment, was performed to find how much these moments contribute to recognizing the main features acquired with the CCD's sensor.

The measurements have shown that computing two to four principal components was sufficient to explain 55% to 80% of the original data, and either the first or fourth moments were contained in two and four principal components.

Despite seven invariant moments being used, such analysis led to the conclusion that when using 4 principal components, one may achieve the explanation of 80% for the original data, with low error, as well as, not a significative variation.

Besides, considering the better arrangement of features, i.e., PC2 and PC4, it is possible to observe the performance in

computing processing. In other words, the gain in performance reaches to 30% compared to the original data.

Finally, support vector machine classifiers have been applied to classify the five different stages of growth of the Fall armyworm.

Concerning the set of SVM classifiers, the results demonstrated the efficiency and innovation of the classification method in the proposed scenario. The results also revealed that the Gaussian kernel function exhibited the best classification accuracy and precision.

The results also have shown that the developed method is capable of helping in the control of one of the main pests of maize crops, the Fall armyworm (Spodoptera frugiperda)

For future works, it is suggested to extend this research to an unsupervised method to reach the selection of the principal components numbers to remain with the semantic features from a recognized agricultural pest.

VI. Acknowledgment

This research was partially supported by the São Paulo Research Foundation (FAPESP 17/19350-2). We thank the Brazilian Corporation for Agricultural Research (Embrapa) and the Post-Graduation Program in Computer Science from the Federal University of São Carlos (UFSCar). The Authors also recognize the helpful discussions with MSc Bruno M. Moreno to finalize the manuscript.

References

[1] A. B. Bertolla and P. E. Cruvinel, "Dimensionality reduction for ccd sensor-based image to control fall armyworm in agriculture," in *2024 ALLSENSORS 9th International Conference on Advances in Sensors, Actuators, Metering and Sensing*. IARIA, 2024, pp. 7–12.

[2] C. Zhang, H. Hu, D. Fang, and J. Duan, "The ccd sensor video acquisition system based on fpga&mcu," in *2020 IEEE 9th Joint International Information Technology and Artificial Intelligence Conference (ITAIC)*, vol. 9. IEEE, 2020, pp. 995–999.

[3] S. Sankaran, R. Ehsani, and E. Etxeberria, "Mid-infrared spectroscopy for detection of huanglongbing (greening) in citrus leaves," *Talanta*, vol. 83, no. 2, pp. 574–581, 2010.

[4] J. L. Miranda, B. D. Gerardo, and B. T. T. III, "Pest detection and extraction using image processing techniques," *International Journal of Computer and Communication Engineering*, vol. 3, no. 3, pp. 189–192, 2014.

[5] C. Ji *et al.*, "Big data processing: Big challenges and opportunities," *Journal of Interconnection Networks*, vol. 13, no. 03n04, p. 1250009, 2012.

[6] W. K. Vong, A. T. Hendrickson, D. J. Navarro, and A. Perfors, "Do additional features help or hurt category learning? the curse of dimensionality in human learners," *Cognitive Science*, vol. 43, no. 3, p. e12724, 2019.

[7] A. L. M. Levada, "Parametric PCA for unsupervised metric learning," *Pattern Recognition Letters*, vol. 135, pp. 425–430, 2020.

[8] F. Anowar, S. Sadaoui, and B. Selim, "Conceptual and empirical comparison of dimensionality reduction algorithms (PCA, KPCA, LDA, MDS, SVD, LLE, ISOMAP, LE, ICA, t-SNE)," *Computer Science Review*, vol. 40, p. 100378, 2021.

[9] S. Ayesha, M. K. Hanif, and R. Talib, "Overview and comparative study of dimensionality reduction techniques for high dimensional data," *Information Fusion*, vol. 59, pp. 44–58, 2020.

[10] K. Pearson, "LIII. On lines and planes of closest fit to systems of points in space," *The London, Edinburgh, and Dublin Philosophical Magazine and Journal of Science*, vol. 2, no. 11, pp. 559–572, 1901.

[11] A. L. M. Levada, "PCA-KL: a parametric dimensionality reduction approach for unsupervised metric learning," *Advances in Data Analysis and Classification*, vol. 15, no. 4, pp. 829–868, 2021.

[12] F. Pan, G. Song, X. Gan, and Q. Gu, "Consistent feature selection and its application to face recognition," *Journal of Intelligent Information Systems*, vol. 43, pp. 307–321, 2014.

[13] S. Nanga *et al.*, "Review of dimension reduction methods," *Journal of Data Analysis and Information Processing*, vol. 9, no. 3, pp. 189–231, 2021.

[14] Z. A. Sani, A. Shalbaf, H. Behnam, and R. Shalbaf, "Automatic computation of left ventricular volume changes over a cardiac cycle from echocardiography images by nonlinear dimensionality reduction," *Journal of Digital Imaging*, vol. 28, pp. 91–98, 2015.

[15] R. M. Wu *et al.*, "A comparative analysis of the principal component analysis and entropy weight methods to establish the indexing measurement," *PLoS One*, vol. 17, no. 1, p. e0262261, 2022.

[16] R. C. Gonzalez and R. E. Woods, *Digital Image Processing*. Pearson Prentice Hall, 2004.

[17] G. Saravanan, G. Yamuna, and S. Nandhini, "Real time implementation of rgb to hsv/hsi/hsl and its reverse color space models," in *2016 International Conference on Communication and Signal Processing (ICCSP)*. IEEE, 2016, pp. 0462–0466.

[18] W. Zhao and J. Wang, "Study of feature extraction based visual invariance and species identification of weed seeds," in *2010 Sixth International Conference on Natural Computation*, vol. 2. IEEE, 2010, pp. 631–635.

[19] L. Zhang, F. Xiang, J. Pu, and Z. Zhang, "Application of improved hu moments in object recognition," in *2012 IEEE International Conference on Automation and Logistics*. IEEE, 2012, pp. 554–558.

[20] K. Hongyu, V. L. M. Sandanielo, and G. J. de Oliveira Junior, "Principal analisys components: teorical summart, aplication and interpretation, (análise de componentes principais: resumo teórico, aplicação e interpretação)," *E&S Engineering and Science*, vol. 5, no. 1, pp. 83–90, 2016.

[21] B. Zhao, X. Dong, Y. Guo, X. Jia, and Y. Huang, "PCA dimensionality reduction method for image classification," *Neural Processing Letters*, pp. 1–22, 2022.

[22] M. P. Uddin, M. A. Mamun, and M. A. Hossain, "PCA-based feature reduction for hyperspectral remote sensing image classification," *IETE Technical Review*, vol. 38, no. 4, pp. 377–396, 2021.

[23] B. M. S. Hasan and A. M. Abdulazeez, "A review of principal component analysis algorithm for dimensionality reduction," *Journal of Soft Computing and Data Mining*, vol. 2, no. 1, pp. 20–30, 2021.

[24] P. E. Hart, D. G. Stork, R. O. Duda *et al.*, *Pattern classification*. Wiley Hoboken, 2000.

[25] S. Haykin, *Neural Networks: A Comprehensive Foundation*. Prentice Hall PTR, 1998.

[26] K. Faceli, A. C. Lorena, J. Gama, T. A. d. Almeida, and A. C. P. d. L. F. d. Carvalho, "Inteligência artificial: uma abordagem de aprendizado de máquina," 2021.

[27] M. A. Hearst, S. T. Dumais, E. Osuna, J. Platt, and B. Scholkopf, "Support vector machines," *IEEE Intelligent Systems and their Applications*, vol. 13, no. 4, pp. 18–28, 1998.

[28] A. C. Lorena and A. C. De Carvalho, "Uma introdução às support vector machines," *Revista de Informática Teórica e Aplicada*, vol. 14, no. 2, pp. 43–67, 2007.